RSC Advances

ROYAL SOCIETY OF CHEMISTRY

www.rsc.org/advances

RSC Advances

Article

A simple and dual responsive efficient new Schiff base chemoreceptor for selective sensing of F⁻ and Hg²⁺: application to bioimaging in living cells and mimicking of molecular logic gates†

Additi Roy Chowdhury,[ab] Pritam Ghosh,[a] Biswajit Gopal Roy,[c] Subhra Kanti Mukhopadhyay,[d] Partha Mitra[e] and Priyabrata Banerjee*[ab]

A novel colorimetric hydrazine-functionalized Schiff base chemoreceptor, NPMP, was synthesized following a simple one-step Schiff base condensation pathway. NPMP showed selective colorimetric change from faint yellow to yellowish orange in presence of biologically ubiquitous fluoride (F⁻). It also showed a '*turn off*' fluorescent response in the presence of F⁻ that could effectively distinguish it from all anions tested except acetate. Acetate (OAc⁻) showed a weak response, while other anions like chloride, bromide, iodide, phosphate, hydrogen sulfate and nitrate did not have any observable effect on the NPMP receptor (E)-4-nitro-2-((2-(perfluorophenyl)hydrazono)methyl)phenol. Recognition of F⁻ in the presence of NPMP can be explained in light of multiple H-bonding interactions, as well as acid-base interactions between host receptor and guest F⁻. Interestingly, NPMP also showed enormous potential as a staining agent in determining the presence of low levels of intracellular fluoride. Moreover, it was found that in NPMP ···· F⁻ solutions, incorporation of Hg²⁺ showed observable optical changes, revealing that this compound is a smart material. Optical responses of NPMP can mimic a molecular logic gate (INHIBIT gate). This can be interpreted as a combination of AND gate with a NOT function. It also represented a potential 'Write-Read-Erase-Read' memory function reflecting multi-writing ability.

Introduction

There is increasing interest in the determination of inorganic anions and heavy metal ions owing to their huge impact on biology and the environment, therefore development of chemoreceptors for selective sensing and recognition of biologically important anions and heavier metals are of major concern.[1-5] While the growth of cation receptors have seen great success in the last few decades, anion receptor chemistry has received much less attention, and the development of suitable chemoreceptors for selective detection of anions and heavy metals remain a challenging endeavor.[5b] F⁻ is one such important anion because of its unique properties and its enormous role in matters related to health, medicine and the environment.[6-7] It is well known that F⁻ is present in many hypnotics and in psychiatric drugs.[8] However its presence in excess amounts in the human body is responsible for ill-effects like osteoporosis,

osteoarthyritis, fluorosis and immune system disruption.[9-12] Several methods like ion chromatography, ion-selective electrodes, willard and winter methods are used for quantitative detection of fluoride.[13] However, all of these processes are costly and complicated. Therefore, the development of cost-effective and readily accessible optical chemoreceptors for fluoride recognition have drawn considerable attention in supramolecular chemistry.[9,14] To date, several neutral anion-binding receptors featuring organic heterocycles like pyrrole, pyridine, indole and other structural units like amides and amines, which are well known H-bond donors, have been incorporated in receptor sites.[15] To the best of our knowledge, only a few research groups are working in this area of anion recognition with organic Schiff bases bearing functional groups like –OH in their binding site.[16,17] These factors motivate us to develop a new Schiff base chemoreceptor (NPMP) with interacting sites involving –OH and –NH functionalities. In order to see the substitution affect in the receptor backbone, a nitro group is incorporated in the aromatic ring. The presence of the nitro substituent increases the electron deficiency in the scaffold, which in turn facilitates F⁻ sensing.[18] Furthermore the receptor···F⁻ adduct shows interesting spectral changes in presence of Hg²⁺, while other competing cations are unresponsive.[5c] Owing to the toxicity of heavier transition-metal ions, the development of sensitive chemoreceptors like NPMP for their selective detection is also of significant importance. In this context, Hg²⁺ is one such heavier metal that is hazardous to the environment because it can be widely distributed in air, water and soil. Finally, this novel receptor also has profound application as a fluorescent staining agent for detection of F⁻ inside pollen grains of Techoma stans and in cells of the diploid fungus Candida albicans.

Experimental

Materials

All starting materials (chemical reagents, solvents) were obtained commercially and were of analytical grade. Solvents, including methanol and diethyl ether, were received from Merck India Pvt. Ltd and used without purification. All tetrabutyl ammonium salt of anions like fluoride (hydrate), chloride, bromide, iodide, nitrate, hydrogen sulfate, acetate and phosphate were purchased

from Sigma Aldrich chemical company and used as received. DMSO and HEPES-Buffer were of spectroscopic grade, and were purchased from Merck India Pvt. Ltd. and used without purification.

Apparatus

Infrared spectra were recorded on an ATR-FT-IR (Model-Alpha, Bruker, Germany) instrument. A Perkin Elmer 2400C elemental analyser was used to collect the microanalytical (C, H, N) data. Mass spectra were obtained from Advion's CMS Expression (serial number: 3013-0140) compact mass spectrometer. ^{1}H-NMR spectra were recorded on a Bruker AV-400 spectrometer. UV–Vis spectra were taken on ALS-SEC2000 and Agilent Cary 60 spectrophotometers. An MBraun glove box was used for sample preparation. Fluorescence titration experiments were done on a Perkin Elmer LS-45 spectrometer. Fluorescence imaging experiments of bio cells were performed where the imaging system comprised of a fluorescence microscope (Leica DM 1000 LED), digital compact camera (Leica DFC 420C) and an image processor (Leica Application Suite v3.3.0). The microscope was equipped with a mercury 50 watt lamp.

Results and Discussion

Synthesis and characterization

Preparation of **NPMP**: Pentafluorophenyl-hydrazine (1mmol, 0.198g) was dissolved in 15mL of stirred methanol. 2-Hydroxy-5-nitro benzaldehyde (1mmol, 0.167g) was dissolved in a separate vessel in 5mL of methanol, and this solution was added dropwise to the stirred solution of Pentafluorophenyl-hydrazine. The solution was stirred for six hours at room temperature (rt). A yellow precipitate appeared which was collected and washed several times with ether in small fractions (Scheme 1). Layering of the compound in 1:1 methanol/ether, yielded X-ray quality single crystals after one week of slow diffusion of a methanol solution into ether followed by slow evaporation of the methanol/ether mixture. The formation of pale yellow crystalline material **NPMP** was confirmed by elemental analyses, FT-IR (S1, ESI†), single crystal X-Ray (Table S1-S4, ESI†) and also by solution-state techniques like ESI-MS, ^{1}H NMR and UV-Visible studies (Fig. S2-S3, S5 ESI†). Elemental analysis for **NPMP**: Calc. $C_{13}H_6N_3O_3F_5$: C: 44.9%; H: 1.7%; N: 13.8%; found. C: 44.8%; H: 1.65; N: 13.72%. Yield: (0.32 g, 92%); mp. 202°C; m/z Calcd. 347 for $C_{13}H_6N_3O_3F_5$: found for [m/z, negative mode (**NPMP**-H$^+$), in MeOH] 345.81. ^{1}H-NMR (400 MHz, DMSO-d$_6$, Me$_4$Si) δ = 7.067 (d, 1H), 8.121 (q, 1H), 8.431 (s, 1H), 8.47 (d, 1H), 10.682 (s, NH), 10.682 (s, OH).
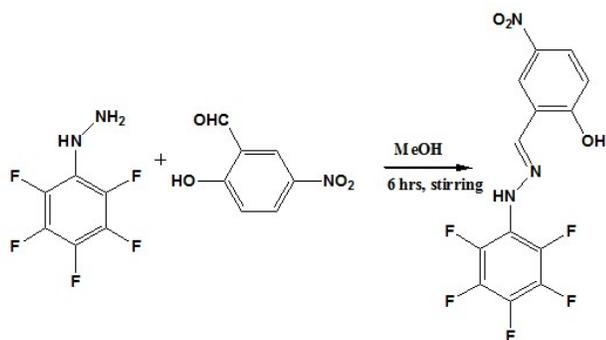

Scheme 1. Synthesis of the receptor **NPMP**.

ORTEP and atom numbering Scheme of **NPMP** is shown in Fig. 1a and intermolecular and intramolecular H-bonding is shown in Fig. 1b.

X-Ray Crystal Structure

X-ray quality single crystals of **NPMP** are obtained from slow diffusion of methanol into ether and followed by slow evaporation. **NPMP** crystallized in the P2(1)/c space group. Four **NPMP** moieties are present in the unit cell and form a closely packed structure along the crystallographic *a* axis. Intra and inter molecular H-bonding make the whole scaffold planar. Intramolecular H-bonding is present between the
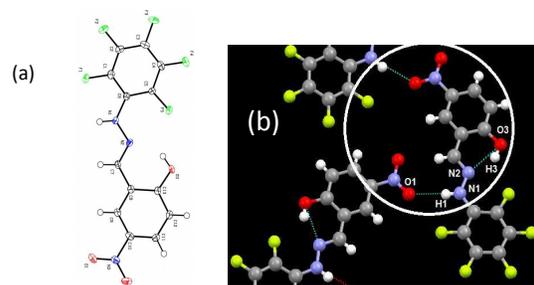
Colour Code: Red: Oxygen; Blue: Nitrogen; Grey: Carbon; White: Hydrogen; Green: Fluorine

Fig. 1 (a) ORTEP with atom numbering for receptor **NPMP**; (b) Segmented view of intermolecular and intramolecular H-bonding interactions in **NPMP**.

imine nitrogen and the hydroxyl hydrogen of the receptor molecule, which is about 1.92 Å and makes a six membered network. The intermolecular H-bonding is present between the nitro oxygen of one receptor molecule and the NH hydrogen of another. The propagation through intermolecular H-bonding forms a supramolecular zig-zag 1D chain (Fig. S4, ESI†). The C=N distance (C7-N2: 1.288 Å) is slightly greater than in an ideal case (1.27 Å). [8, 30, 45] The other bond distances of the ring structure i.e.; C-C (C7-C8: 1.447 Å), C-C (aromatic) (C8-C13:1.434 Å), C-O (C13- O3:1.346 Å) and O-H (0.82 Å) also deviate from the respective ideal bond distances: C-C (aromatic) = 1.54, C-O = 1.35, C-C = 1.43 and O-H = 0.96 Å, suggesting delocalisation of electrons throughout the six-membered ring structure.

Solution state analysis

The sensing ability of receptor **NPMP** towards incoming anions such as F$^-$, Cl$^-$, Br$^-$, I$^-$, HSO$_4^-$, OAc$^-$, NO$_3^-$ and H$_2$PO$_4^-$ were examined by different methods like visual colorimetric changes after addition of anions (instant effect), UV-Visible spectral responses, fluorescence on-off studies and ^{1}H-NMR titration with respective anions.

Visual detection

Visual inspection of receptor **NPMP** solution in DMSO: HEPES buffer (9:1 *v/v*) solvent mixture in the presence and absence of TBA salts of different anions show remarkable changes in the specific cases presented in Fig. 2. For F$^-$, there is a sharp change in color from faint yellow to yellowish orange. In the case of OAc$^-$ the change is very weak, even after addition of excess OAc$^-$. The addition of other anions as TBA salts did not show any visually detectable changes.
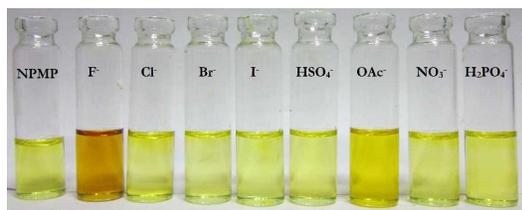
Fig. 2 Solutions of **NPMP** in DMSO-HEPES buffer (9:1 *v/v*) at pH 7.4 in the presence of TBA salts of the anions shown.

UV-Vis titration experiments

The response in optoelectronic properties of **NPMP** to the gradual addition of tetrabutyl ammonium fluoride (TBAF) was investigated by UV-Vis titration experiments. In DMSO-HEPES buffer (9:1 *v/v*) medium, the titration experiments were carried out for receptor **NPMP** (2×10^{-5}M) with an incremental addition of TBAF (0-2eq). The result of the spectrophotometric titration experiment is shown in Fig. 3. In the absence of TBAF, the absorption profile of receptor **NPMP** shows π-π* and n-π* transitions in the 200-350 nm window (Fig. S5, ESI†);[19] there is hardly any tangible transition within the visible region. The transition at 300 nm is responsible for electronic transitions localized on the azomethine group (C=N).[19,20] The next low-energy shoulder at 330 nm is perhaps due to an n-π* transition within the skeletal framework.[21,22] On addition of TBAF, an immediate color change of the solution was observed. By UV-Vis analysis, a new absorption peak was detected with increasing addition of F⁻ ion. This red-shifted peak at 435 nm can be assigned as a charge-transfer transition within the scaffold. Proton abstraction from the –OH unit will build up negative charge on the oxygen center (*vide infra*, eq. 1), which in turn will facilitate enhancement of ICT.[21-23] Incorporation of electron-withdrawing chromophores like -NO₂ led to low-energy electron transfer in the system.[24] Upon successive addition of F⁻ ions (from 0 to 2.0 equiv), the intense peaks at 300 and 330 nm were gradually bleached, while new peaks at 365 nm and 435 nm gradually increased in intensity. The binding constant of **NPMP** with F⁻ has been found to be 4.4×10^3M⁻¹ (Fig. S6, ESI†).

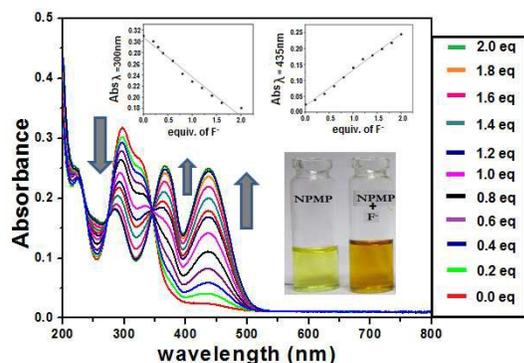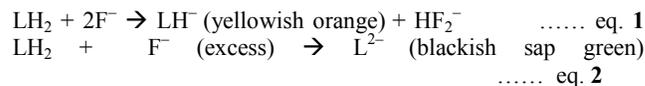**Fig. 3** UV-Vis spectral changes of **NPMP** (2×10^{-5}M) with (2×10^{-4}M)TBAF (0-2eq) in DMSO-HEPES buffer (9:1 *v/v*) at pH 7.4; inset: Color of ligand in the presence (right) and absence (left) of F⁻.

Sequential addition of excess F⁻ (up to 25 equivalents) led to a sharp color change from yellow (LH₂) to blackish sap green (L²⁻), which was not stable enough for further studies (*vide* eq. 2, Fig. 4). However, we were fortunate enough to collect the absorption spectrum profile of the L²⁻ species, which shows a broad shoulder at 600 nm due to the improved ICT inside the doubly deprotonated receptor L²⁻. The initial sap green color returned to the more stable LH⁻ species within a few seconds. This is possibly due to the presence of moisture from the atmosphere, which facilitates the protonation of L²⁻ to LH⁻.

$$LH_2 + 2F^- \rightarrow LH^- \text{ (yellowish orange)} + HF_2^- \quad \dots\dots \text{ eq. } \mathbf{1}$$
$$LH_2 + F^- \text{ (excess)} \rightarrow L^{2-} \text{ (blackish sap green)} \quad \dots\dots \text{ eq. } \mathbf{2}$$

Consistent with this hypothesis, the same experiment, when performed inside an argon-containing glove box, produced the L²⁻ species with improved stability due to the low levels of moisture inside the glove box (<1ppm).
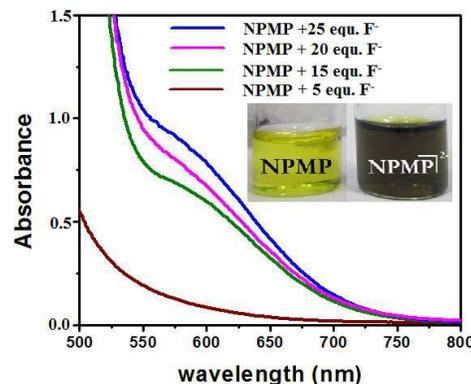

Fig. 4 UV-Vis response of **NPMP** (2×10^{-5}M) with excess F⁻ in DMSO-HEPES buffer (9:1 v/v) at pH 7.4.

The addition of the other anions Cl⁻, Br⁻, I⁻, HSO₄⁻, NO₃⁻ and H₂PO₄⁻ showed no detectable response by UV-Vis even with excess anion (Fig. S7a, ESI†). The results of an interference study is shown in Fig. S7b, ESI†. On the other hand, OAc⁻ shows a weak response (Fig. S8, ESI†).

Development of 2 and 3 input logic gate

Introduction of anionic and cationic input modes can reflect a distinct change in the UV-Vis absorption spectrum. The sensitive absorbance responses (viz. selective anions/cations) of **NPMP** motivated us to fabricate Boolean logic gates and arithmetic calculation at the molecular level.[25] A combinational logic circuit was constituted of AND and NOT circuits at the molecular level by proper utilization of F⁻ and Hg²⁺ as chemical inputs. The UV-Vis spectral response of **NPMP** (2×10^{-5}M) in the presence of one input F⁻ (2×10^{-4}M) will produce an output at 435 nm. The absorbance output of this spectral response is mimicking the AND logic gate function. Interestingly, the absorbance output (435 nm) here is noticed in the presence of F⁻ (2×10^{-4}M), where receptor **NPMP** and F⁻ are considered as inputs (*viz.* In 1 and In 2). The output will be considered as HIGH (i.e., 1) if input is also HIGH (i.e., 1), which means that if the inputs (In 1 and In 2) are 'ON' then output is also 'ON' otherwise it will be 'OFF' [i.e., the output response at 435 nm will appear if input In 1 (**NPMP**) and In 2 (F⁻) are both present together].[26,27] The results are best fitted as an AND logic gate function. A simplified logic symbol is shown in Fig. 5a, where In 1 and In 2 as inputs are shown along with the output Y (Table 1).

On the other hand, a three-input combinational circuit could be executed where Hg²⁺ (10^{-4}M) as a third input (In 3) will be considered that will inhibit the absorbance output of In 1 and In 2. Therefore, in presence of chemical input Hg²⁺(10^{-4}M), the

output signal (*i.e.;* 1, ON state) at 435 nm is minimized, which, according to Boolean arithmetic, will become 0 (OFF state).[25-28]

Table 1 AND gate for receptor **NPMP** at 435 nm		
Inputs		Output (λ=435 nm)
In1 (**NPMP**)	In 2 (F$^-$)	Y
0	0	0
1	0	0
0	1	0
1	1	1

Table 2 INHIBIT gate for receptor **NPMP** at 435 nm			
Inputs			Output (λ=435 nm)
In1 (**NPMP**)	In 2 (F$^-$)	In 3 (Hg^{2+})	Y
0	0	0	0
1	0	1	0
0	1	0	0
1	1	1	1

The 'OFF' outset is possibly due to formation of HgF$_2$ species, which, in turn, is responsible for the presence of free **NPMP** receptor in the reaction solution (Fig. S9, ESI†). However, the same experimentation with other cations such as Bi^{3+}, Al^{3+}, Cr^{3+}, Mn^{2+}, Zn^{2+}, Cd^{2+}, Fe^{2+}, Fe^{3+} and Co^{3+} did not show any detectable changes. Output is available when In 2 (F$^-$) is in the ON mode *i.e.,* upon interaction between input 2 (F$^-$) (2 x 10^{-4}M) and the receptor **NPMP** (2x10^{-5}M), a significant enhancement of the 435 nm peak is observed. Subsequent addition of input 3 (Hg^{2+}) will return the system to (output Y) the zero state (OFF). This is NOT gate. In accordance with truth Table 2, combination of all inputs resulted in the vanishing of the 435 nm peak, which may be interpreted as output 0. Systematic monitoring of the UV-Vis response at 435 nm followed by sequential addition of F$^-$ (input 2) and Hg^{2+} (input 3), one after the other, leads to an INHIBIT logic gate function (Fig. 5b). Interestingly, this type of reversible colorimetric switch ON-OFF could be repeated several times by alternate addition of F$^-$ and Hg^{2+} to the **NPMP** receptor solution (Fig. 5e and Fig. S10, ESI†). Nowadays, these sorts of reversible switches are of immense importance because of their considerable impact on the realm of information technology. Development of a sequential logic circuit displaying "Write-Read-Erase-Read" sequences in line with binary logic functions is depicted in Fig. 5c. In this present molecular logic gate operation, the strong absorption at 435 nm can be presented as the ON state (OUT = 1) whereas the OFF state can be labeled as a very weak absorption at the same wavelength (OUT = 0). Two chemical inputs, F$^-$ (In 2) and Hg^{2+} (In 3), are defined as Set (S) and Reset (R), respectively. In the high input state (S = 1) the whole system is in a state of write and memorize. Contrariwise, the stored information can be erased by the Reset input, reflecting writing and memorization of a 0 binary set. The feedback loop is actually a representation of reversible and reconfigurable sequences of Set/Reset logic operations. The reversible and reconfigurable sequences of Set/Reset logic operations are represented by a feedback loop (*vide infra*, Fig. 5d). Schiff bases of this kind with dual response, without any appreciable degradation in optical output stage up to a considerable number of cycles, might be an asset for consideration as a potential molecular logic device feedstock. In the future, there are bright prospects for exploring new avenues in this realm.
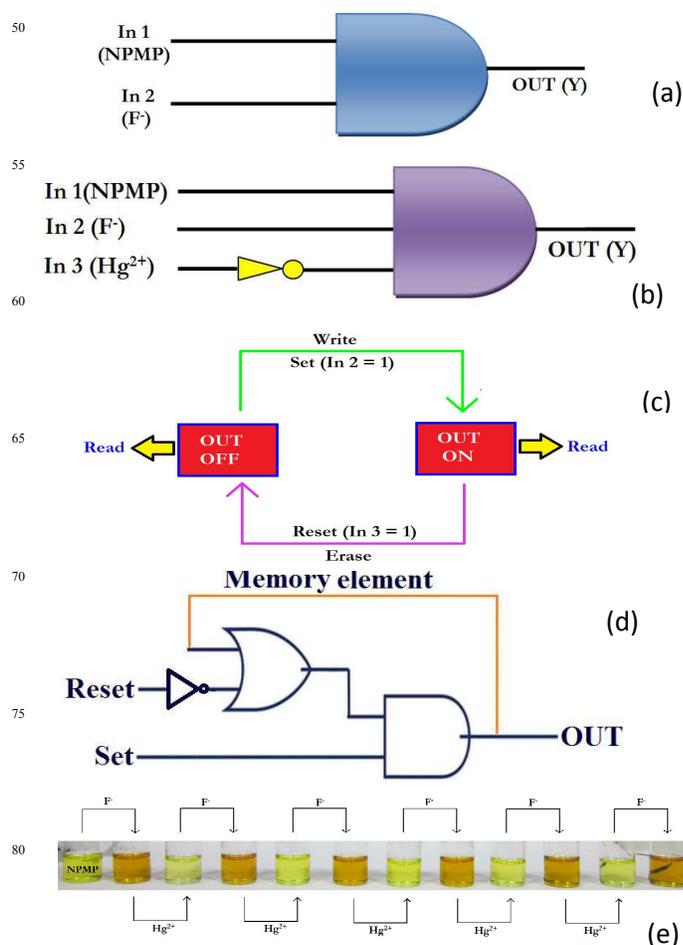

Fig. 5 The logic circuit for (a) AND and (b) INHIBIT logic gate (c) proposed loop demonstrating the reversible logic operations with 'Write–Read–Erase–Read' function (d) logic circuit with memory unit (e) colorimetric response after every sequential addition of F$^-$ (2 x10^{-4}M) and Hg^{2+} (10^{-4}M) ions.

Spectrofluorimetric titration with TBA$^+$F$^-$

In the **NPMP** receptor, intramolecular H-bonding between the imine nitrogen and the skeletal hydroxyl proton reduces the process of isomerization, where imine –C=N rotation is restricted, which prevents non-radiative deactivation of the excited state.[29] The intramolecular H-bonding is quite strong, which is due to presence of an electron-withdrawing (-NO$_2$) group in the fluorophore site of this chemoreceptor.[30] However, on addition of TBAF, this H-bonded network will likely be disrupted, and proton abstraction from the hydroxyl group will occur. Therefore, the conformational restriction of –C=N isomerisation is now removed, which in turn will reduce the rigidity of the system and make non-radiative decay possible from the excited state, and hence fluorescence quenching (Fig. 6a).[24,29] Sequential addition of F$^-$ and Hg^{2+} in the same receptor solution will give rise to emission quenching and enhancement, respectively (Fig. S11, ESI†).

In order to determine the stoichiometry of the **NPMP** with F$^-$, a series of solutions containing 4x10^{-5} M of TBAF and 4x10^{-5} M of **NPMP** was prepared in DMSO, such that the total concentration of the resultant solution remains constant. The mole fraction of the anion varied from 0.1 to 1.0. The corrected fluorescence at 450 nm is plotted against the mole fraction of the

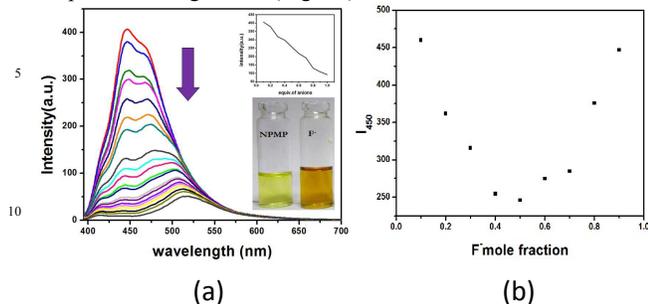anion. The curve shows 1:1 complexation between the host receptor and the guest F⁻ (Fig. 6b).

(a)   (b)

Fig. 6 (a) Spectrofluorimetric titration of NPMP (2 x 10^{-6} M) with 0 to 2 eq of TBA⁺F⁻ in DMSO-HEPES buffer (9:1 *v/v*) at pH 7.4; (b) Job's plot of receptor with F⁻ anion with a total concentration of 4 x 10^{-5} M.

Detection limit calculation

The detection limit (DL) has been calculated following fluorescence titration.[31] The fluorescence emission spectrum of NPMP was repeated 10 times, and its standard deviation was measured. The limit of detection (LOD) is calculated from the following formula:

$$DL = 3\sigma/k$$

where σ is the standard deviation of the blank solution of NPMP. Gradual enhancement of NPMP emission intensity at 450 nm during fluorimetric titration with TBAF is plotted against its concentration. The slope (k) is derived from this plot (Fig. S12, ESI†). LOD turns out to be 6.6×10^{-6} M.

^{1}H-NMR titration

In order to confirm the mode of interaction between receptor and TBAF, a ^{1}H-NMR titration study was conducted in DMSO-d_6. Initially the –OH protons were slightly shifted downfield with gradual addition of F⁻, supporting the H-bonded network formation in initial stage. However, on further addition of F⁻ the –OH proton intensity diminished rapidly and became broadened. On addition of 1.25 equivalents of F⁻, the –OH proton peak totally disappeared (Fig. 7). Interestingly, it was observed in comparison the –NH proton signal did not reduce much in intensity on addition of F⁻.
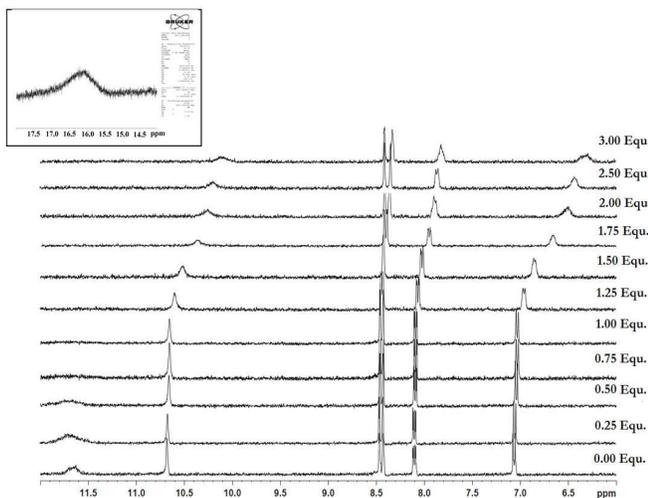

Fig. 7 ^{1}H-NMR titration of NPMP in DMSO-d_6 solvent with a standard solution of TBAF (inset shows the zoomed view of HF_2^- at ~16.1ppm).

Finally, addition upto three further equivalents of F⁻ showed that the –NH proton shifted upfield, facing a higher electron density that strengthens the acid-base type interaction between host NPMP and guest F⁻.[6] TBAF addition (up to 3 equivalents) led to the appearance of a characteristic signal for HF_2^- at 16.1ppm (Fig. 7 inset). This showed that the presence of groups like –NO_2 definitely helped in enhancing the acidity the of –OH and –NH protons, which in turn facilitated HF_2^- formation (Fig. 7).

***In vitro* F⁻ detection**

In vitro F⁻ detection by probes like NPMP is of immense importance for realization of non-skeletal fluorosis. This can affect human soft tissues and multiple organs as well.[6] It is already confirmed that significant interactions of fluoride with NPMP are possible in aqueous organic systems (*vide supra*, UV-Vis and spectrofluorimetric titrations). This interaction motivated us to test their staining ability. Two different types of cells *viz.* Candida albicans (a diploid fungus) and Pollen grains collected from Techoma stans were selected for this purpose (see ESI† for details of the cell studies and cell imaging). After incubation with fluoride, the control cells were visualized under a fluorescence microscope with a UV-filter. The controls did not respond under UV light (Fig. 8a and 8b); however, incubation of the cells for 1 hr with 100 micromolar NPMP resulted in a sparkle-blue emission observed by the UV-filtered fluorescence microscope (Fig. 8c and 8d). The results furthermore suggest that NPMP can be purposefully used as a staining probe in detection of intracellular fluorides from living cells. [32-37]
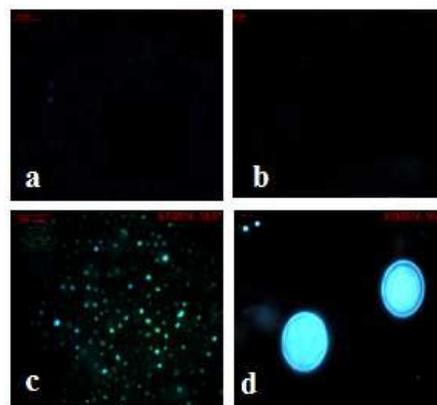

Fig. 8 Fluorescence image of the control cells (a): Candida albicans and (b): Pollen grains of Techoma stans; Detection of F⁻ inside living cells under fluorescence microscope, (c) *Candida albicans* incubated in F⁻ solution and stained with NPMP (d) Pollen grains incubated in F⁻ solution and stained with NPMP.

Conclusion

In summary, colorimetry and fluorescence dual-channel recognition for selective detection of F⁻ and also of Hg^{2+} heavy-metal ion was explored. The receptor is structurally characterized and receptor····guest F⁻ interactions have been fully established using physico-chemical and numerous spectroscopic techniques.

The receptor **NPMP** recognizes F⁻ selectively in the presence of other contending anions with distinct colorimetric change. Furthermore, in solution the NPMP receptor···· F⁻ adduct can selectively recognize Hg^{2+} metal ion in the presence of other competing metals. Through fluorescence imaging studies, we established that this receptor is potentially a very useful probe as a staining agent for detection of low-level intracellular fluoride in living cells. All these positive findings motivate us for further development of other small but smart organic receptors enriched with optoelectronic properties that will have enormous potential in biomedical application.

Acknowledgement

Notes and references

[a] Surface Engineering & Tribology Group, CSIR-Central Mechanical Engineering Research Institute, Mahatma Gandhi Avenue, Durgapur-713209, WB, India. Fax: +91-343- 2546 745; Tel: +91-343-6452220; E-mail: _pr_banerjee@cmeri.res.in_ and _priyabrata_banerjee@yahoo.co.in_ Webpage: www.cmeri.res.in and www.priyabratabanerjee.in
[b] Academy of Scientific and Innovative Research at CSIR-CMERI, Durgapur 713209,India.
[c] Department of Chemistry, Sikkim University, Gangtok-737102, Sikkim, India.
[d] Department of Microbiology, The University of Burdwan, Burdwan-713104, India.
[e] Indian Association for the Cultivation of Science, Jadavpur, Kolkata 700032, India.

†Crystallographic details, UV-Vis**,** ESI-MS, ¹H-NMR and FT-IR of **NPMP** are provided. Crystallographic data of structure **NPMP** reported in this article are available in the Cambridge Crystallographic Data Centre as deposition No. CCDC: 1015470 .Supplementary data associated with this article can be found in the online version, See DOI: 10.1039/b000000x/

References

1 V. Amendola, D. Esteban-Go'mez, L. Fabbrizzi and M. Licchelli, *Acc. Chem. Res.*, 2006, **39**, 343.
2 P. D. Beer and P. A. Gale, *Angew. Chem. Int. Ed.*, 2001, **40**, 486.
3 P. Banerjee, A. D. Jana, G. Mostafa and S. Goswami, *Eur. J. Inorg. Chem.*, 2008, 44.
4 S. Das, P. Banerjee, S-M Peng, G-H Lee, J. Kim and S. Goswami, *Inorg. Chem.*, 2006, **45**, 562.
5 (a) P. A. Gale, *Coord. Chem. Rev.*, 2003, **240**, 191; (b) R. Arabahmadi, M. Orojloo and S. Amani, *Anal. Methods*, 2014,**6**, 7384. (c) B. Bag and A. Pal, Org. Biomol. Chem., 2011, **9**, 4467.
6 (a) P. Ghosh, B. G. Roy, S. Mukhopadhyay and P. Banerjee, *RSC Adv.*, 2015, **5**, 27387; (b) A. Roychowdhury, P. Ghosh, S. K. Saha, P. Mitra and P. Banerjee, *Spectrochim. Acta*, *Part A*, 2014, **124**, 492.
7 K. K. Majumdar, *Indian J. Public Health.*, 2011, **55**, 303.
8 S. W. Zhang and T. M. Sager, *J. Am. Chem. Soc.*, 2003*,* **125***,* 3420.
9 S. Sharma, M. S. Hundal and G. Hundal., *Org. Biomol. Chem.*, 2013, **11**, 654.
10 X. Peng, Y. Wu, J. Fan, M. Tian and K. Han, *J. Org. Chem.*, 2005, **70**, 10524.
11 R. M. F. Batista, E. Oliveira, S. P. G. Costa, C. Lodeiro, M. Manuela, and M. Raposo, *Org. Lett.*, 2007, **9**, 3201.
12 M. Kleerekoper, *Endocrinol. Metab. Clin. North Am.*, 1998, **27**, 441.
13 (a) J-T. Yeh, P. Venkatesan and S-P. Wu, *New J. Chem.*, 2014,**38**, 6198; (b) W. D. Armstrong, *J. Am. Chem. Soc.*, 1933, **55**, 1741; (c) R. I. Stefan, J. F. van Staden and H. Y. Aboul-Enein, *Pharm. Acta Helv.*, 1999, **73**, 307; (d) M. A. G. T. van den Hoop, R. F. M. J. Cleven, J. J. van Staden and J. Neele, *J. Chromatogr. A*, 1996, **739**, 241.
14 A. K. Mahapatra, S. K. Manna and P. Sahoo, *Talanta*, 2011, 2673.
15 Q. Li, Y. Guo, J. Xu and S. Shao, *J. of Photochem and Photobiol.*, 2011, **103**, 140.
16 D. Sharma, S. K. Sahoo, S. Chaudhury, R. K. Bera and J. F. Callan, *Analyst*, 2013, **138**, 3646.
17 R. Sivakumar, V. Reena, N. Anonthi, M. Babu, S. Anandan and S. Velmathi, *Spectrochim. Acta, Part A*, 2010, **75**, 1146
18 X. –F. Shang, *Spectrochim. Acta, Part A,* 2009, **72**, 1117.
19 P. Ghosh, A. Roychowdhury, S. K. Saha, M. Ghosh, M. Pal, N. C. Murmu and P. Banerjee, *Inorg. Chim. Acta*, 2015, **429**, 99.
20 S. Devaraj, D. Saravanakumar and M. Kandaswamy, *Sens. Actuators, B*, 2009, **136**, 13.
21 A. A. Gabr, *Spectrochim. Acta*, *Part A*, 1990, **46**, 1751.
22 A. J. Zare and P. Ataeinia, *Life. Sci. J.*, 2012, **94**, 2396.
23 H. Yang, H. Song, Y. Zhu and S. Yang, *Tetrahedron Lett.*, 2012, **53**, 2026.
24 V. Bhalla, R. Tejpal and M. Kumar, *Tetrahedron*, 2011, **67**, 1266.
25 M. Irie, *Chem. Rev.*, 2000, **100**, 1685.
26 J. Millman and A. Grabel, Microelectronics, McGraw-Hill, New York, 1988, ch. 6.
27 M. M. Mano and C. R. Kime, Logic and Computer Design Fundamentals, Prentice-Hall, Upper Saddle 5 River, 4th edn, 2000.
28 B. L. Feringa, Molecular Switches, Wiley-VCH Express, New York, 2001, 37.
29 J. Wu, W. Liu, J. Ge, H. Zhang and P. Wang, *Chem. Soc. Rev.*, 2011, **40**, 3483.
30 X. Zhuang, W. Liu, J. Wu, H. Zhang and P. Wang, *Spectrochim. Acta*, *Part A*, 2011, **79**, 1352.
31 A. Gogoi, S. Samanta and G. Das, *Sens. Actuators*, *B*, 2014, **202**, 788.
32 C. Kar, S. Samanta, S. Mukherjee, B. K. Datta, A. Ramesh and G. Das, *New J Chem.*, 2014, **38**, 2660.
33 S. Sen, M. Mukherjee, K. Chakraborty, I. Hauli, S. K. Mukhopadhyay and P. Chattopadhyay, *Org. Biomol. Chem.*, 2013, **11** 1537.
34 A. Sahana, A. Banerjee, S. Guha, S. Lohar, A. Chattopadhyay, S. K. Mukhopadhyay and D. Das, *Analyst*, 2012, **137**, 1544.
35 S. Guha, S. Lohar, A. Sahana, A. Banerjee, D. A. Safin, M. G. Babashkina, M. P. Mitoraj, M. Bolte, Y. Garcia, S. K. Mukhopadhyay and D. Das, *Dalton Trans.*, 2013, **42**, 10198.
36 A. Sahana, A. Banerjee, S. Lohar, A. Banik, S. K. Mukhopadhyay, D. A. Safin, M. G. Babashkina, M. Bolte, Y. Garcia and D. Das, *Dalton Trans.*, 2013, **42**, 13311.
37 A. Banerjee, A. Sahana, S. Das, S. Lohar, B. Sarkar, S. K. Mukhopadhyay, J. S. Matalobos and D. Das, *Dalton Trans.*, 2013, **42**, 16387.